Two- and Three-Dimensional Ultrastructures of the Micron-Scale Adhesive Setae of a Leaf Beetle *Chrysochus chinensis* (Coleoptera: Chrysomelidae)[1]

Zheng Liu and Ai-Ping Liang[2,3]

Hebei Key Laboratory of Animal Diversity, Langfang Normal University, 100 Aimin West Road, Anci District, Langfang, Hebei 065000, P.R. China

J. Entomol. Sci. 60(1): 1–12 (January 2025)
DOI: 10.18474/JES24-06

Abstract *Chrysochus chinensis* (Baly) (Chrysomelidae: Eumolpinae) is a phytophagous leaf beetle that excels in climbing on its host plants' leaf surfaces and has well-developed adhesive setae on its feet. Using scanning electron microscopy, we examined the ultrastructure of the adhesive setae and recognized three types of setae, namely pointed, spatulate, and discoidal. The terminal plate areas of the three types of setae were 7.59 ± 1.76 μm^2, 41.16 ± 1.46 μm^2, and 63.65 ± 2.35 μm^2, respectively. The three-dimensional topography of the terminal plates of three types of setae were imaged with an atomic force microscope. We found that the terminal plate of the discoidal seta had a concave center and a high circular edge, and the edge was 200–400 nm higher than the center. The ventral side of the spatulate seta was smooth with a 200-nm-high edge at two sides of the terminal plate. The results showed that the discoidal seta had the biggest terminal plate area (63.65 ± 2.35 μm^2) and its topography can gather liquid and produce a 200- to 400-nm-thick fluid film between the terminal plate and smooth substrates. With the help of capillary force of the tarsal secretion, it can enhance adhesion force. The function of the discoidal seta, which is only present on male beetles, is hypothesized to serve for strong attachment force during mating.

Key Words adhesive seta, atomic force microscope, ultrastructure, elytra epidermis

The attachment ability of insects on smooth substrates has attracted considerable interest since the beginning of the study of the natural sciences. Many insects are capable of walking on a vertical wall, glass, or other smooth surfaces with the help of the adhesion force generated by their feet (Gorb and Beutel 2001, Walker 1993). In some cases, the adhesion force of insects can reach up to 100 times their body weight (Vogel and Steen 2010). The tiny adhesive devices on insects' feet play a major role in the attachment process, and they are usually located on the distal part of legs, such as tibia, tarsus, or pretarsus (Gorb 2001, Beutel and Gorb 2001). Throughout evolution, insects have developed two entirely different mechanisms for

---

[1] Received 17 January 2024; accepted for publication 12 March 2024.

[2] Corresponding author (email: liangap@ioz.ac.cn; apliang2020@163.com; ORCID: https://orcid.org/0000-0001-6249-1704).

[3] Tianjin Key Laboratory of Conservation and Utilization of Animal Diversity, College of Life Sciences, Tianjin Normal University, 393 Binshuixidao Road, Xiqing District, Tianjin 300387, P. R. China; Key Laboratory of Zoological Systematics and Evolution, Institute of Zoology, Chinese Academy of Sciences, 1 Beichen West Road, Chaoyang District, Beijing 100101, P. R. China.

attachment—“smooth” and “hairy” (Gorb 2001). The smooth adhesive devices are composed of sacculate and soft materials, such as smooth arolium in Hymenoptera, smooth pulvilli in Cicadellidae and Pentatomidae, and smooth euplantulae in Orthoptera (Federle et al. 2001, 2002; Goodwyn et al. 2006; Orivel et al. 2001; van Casteren and Codd 2010). The hairy adhesive devices are pads covered with hair (setae). These devices are classified into different types according to their distribution and morphology, that is, hairy pulvilli in Diptera, a fossula spongiosa in Reduviidae, and hairy adhesive soles of tarsomeres in Coleoptera (Betz 2003, Beutel and Gorb 2001, Bullock and Federle 2011b, Gorb 1998, Pelletier and Smilowitz 1987, Stork 1980, Stork and Evans 1976, Weirauch 2007, Wigglesworth 1987).

In many Coleoptera, there are amounts of microscale adhesive setae on the ventral side of the tarsus. Each seta consists of two parts: a long setal shaft and an expanded terminal plate. On the basis of the shape of terminal plates, these setae are classified into different types. Diverse adhesive setae have been found in different groups of Coleoptera, and even one species may have several different setal types (Betz 2003, Bullock and Federle 2011b, Liu and Liang 2013, Pelletier and Smilowitz 1987, Stork 1980, Stork and Evans 1976). The terminal plate of an adhesive seta that directly contacts a substrate is a very important ultrastructure in the adhesion process. The Van der Waals force and capillary force between the terminal plate of an adhesive seta and a substrate provides most of the adhesion force (Autumn et al. 2000, Eisner and Aneshansley 2000), so the adhesion force is largely related to the shape, area, and topography of the setal terminal plate. Previous studies usually provided two-dimensional images of the adhesive devices, but the three-dimensional topography was still unknown. To solve this problem, we observed both the two-dimensional ultrastructure and three-dimensional topography of different types of adhesive setae in a leaf beetle *Chrysochus chinensis* (Baly) (Chrysomelidae: Eumolpinae).

Chrysochus chinensis is a medium-sized phytophagous leaf beetle and is extremely good at climbing on leaves or stems. It is widely distributed in the Palearctic realm of East Asia. Adult beetles emerge in middle or late May, reach peak numbers in June, and disappear in early September (Yu et al. 1996). They have complicated diets, primarily feeding on *Cynanchum chinense* R. Brown (Contortae: Asclepiadaceae) and *Ipomoea aquatica* Forsskåi (Tubiflorae: Convolvulaceae) (Jiang 1980). The leaves of *Cy. chinense* are covered with short hairs, and the leaves of *I. aquatica* are relatively smooth without hairs. The hairs on plant leaves have multiple functions including defense against insects by affecting their movement (Gorb and Gorb 2002, Tian et al. 2012). *Chrysochus chinensis* can attach to the surfaces of their host plants or other smooth surfaces with their feet. Thus, it is a suitable research object to investigate the two- and three-dimensional ultrastructures of the adhesive setae.

Atomic force microscopy (AFM) was used to observe the three-dimensional topography of the adhesive setae of *Ch. chinensis*. AFM is a powerful technique that allows the detailed study of surface morphology and mechanical properties of biological materials at the nanoscale or atomic scale (Pettinger et al. 2010). Three AFM imaging modes exist: tapping mode, contact mode, and noncontact mode. The PeakForce quantitative nanomechanical mapping (PF QNM) tapping mode is an advanced tapping mode; images sample topography at very high spatial resolution while simultaneously mapping and distinguishing the nanomechanical properties such as adhesion force, modulus, dissipation, and deformation depth. Of importance, PF QNM is nondestructive to both tip and sample because changes in force are directly used as feedback rather than the oscillation amplitude of the cantilever (Braet et al. 1998, 2001), allowing for accurate measurement of the soft biological hairs used in this experiment.

Materials and Methods

Specimens of investigation. Twenty specimens of *Ch. chinensis*, including 10 male and 10 female beetles, were collected from *Cy. chinense* (Asclepiadaceae) at Olympic Forest Park, Beijing, China in July 2014. The specimens were deposited in the Insect Collection of the Zoological Museum, Institute of Zoology, Chinese Academy of Sciences, Beijing, China.

Scanning electron microscopy (SEM). The tarsi of forelegs, mesolegs, metalegs, and elytra were dissected from the body, cleaned with 2% phosphate-buffered saline, stepwise dehydrated in ascending ethanol concentrations (70%, 80%, 90%, 95%, 100%, ×3), CO_2 critical-point dried, coated with platinum, and then viewed with a Hitachi SU8010 field emission scanning electron microscope (Hitachi Co. Ltd., Tokyo, Japan).

The SEM images were postprocessed with Adobe Photoshop (Adobe Inc.) The area of the tarsi and the length of setae were measured and analyzed using the software package Image-Pro plus 6.0 (Media Cybernetics Inc.). Each part was measured more than three times and averaged.

Atomic force microscopy. For measuring the three-dimensional topography by AFM, untreated tarsi of *Ch. chinensis* were dissected and fixed with the setae lying supinely. The discoidal setae were gently removed by scraping using a thin blade from the center of the first tarsomere of male beetles. The spatulate and pointed setae were separately removed from the third and the first tarsomeres of female beetles. Then these setae were placed into a drop of distilled water on a glass slide. The setae usually clustered together, so they were scattered in water using an insect needle. Then the water was evaporated and dried by heating. In this process the setae were fixed on a glass slide with the help of water. We positioned the setae to measure the surface because the adhesive setae of *Ch. chinensis* were too long and too soft and were easily deformed and disturbed under a very tiny pressure force; the acquired images were unstable and unrepeatable. This method would not destroy the topography of terminal plates. Before measurement we used a high-power optical microscope to preliminarily fix the position of the target seta.

All experiments were conducted under ambient laboratory conditions (temperature: 292 K; air humidity: 46%). Measurement was carried out using a Dimension ICON2-SYS atomic force microscope (Bruker Co. Ltd., Berlin, Germany). Key scan parameters like setpoint, feedback response, and scan rate were automatically selected and constantly adjusted. The model of the AFM probe used was SCANASYST-AIR, which has a triangular silicon nitride cantilever and a rotated symmetric tip. The cantilever used featured a normal spring constant of 0.4 N/m, as well as a normal resonant frequency of 70 kHz. The tip of the probe was equipped with a normal curvature radius of approximately 2 nm.

The surfaces of the discoidal setae were scanned in longitudinal direction. Images of $20 \times 20\ \mu m^2$ area were scanned at 256×256 pixels in a PF QNM tapping mode.

The height sensor signal was used to display the surface image using nanoscope analysis v1.7 (Bruker Nano Surfaces, Santa Barbara, CA).

Results

Ultrastructure of the terminal plates of adhesive setae. We examined the two-dimensional ultrastructures of adhesive hairs (setae) on the ventral surface of tarsi in both male and female *Ch. chinensis* using SEM. *Chrysochus chinensis* had five tarsomeres, with four tarsomeres visible from the ventral side. The first tarsomere of the male *Ch. chinensis* was wider than that of the female beetle. The proximal three tarsomeres that directly contacted the surface during attachment were covered with dense adhesive setae. Each single seta consisted of two parts: a setal shaft and a modified apex (terminal plate). According to the shape of the terminal plates, three different types of setae (pointed, spatulate, and discoidal) were recognized (Fig. 1). Measurements of the three types of adhesive setae of *Ch. chinensis* are listed in Table 1.

These three types of setae were separately situated in specific parts of the tarsus. The three female leg pairs and male metalegs had only two types of setae (Fig. 1G–I), but all three types of setae were present on male forelegs and mesolegs (Fig. 1A–F). The distribution of all three types of setae on male forelegs and mesolegs was indicated with three different colors, with the tapered, spatulate, and discoidal setae highlighted in blue, green, and orange, respectively.

Tapered setae were located on the ventral surfaces of the first and second tarsomeres of the three female leg pairs and the male metalegs (Fig. 1G, H) and were present only at the edge of the first and second tarsomeres of the male forelegs and mesolegs (Fig. 1A, C). This type of seta was straight at the base and tapered upward, 82.01 ± 1.71 ($n = 10$) μm in length and 3.24 ± 0.12 ($n = 10$) μm in width at the base (Fig. 1C). The mean (± SE) area of the terminal plates of tapered setae was 7.59 ± 1.76 ($n = 10$) μm^2. On average the density of the tapered setae was 0.97 ± 0.09 ($n = 10$) per 100 μm^2 area.

Spatulate setae were situated on the ventral surfaces of the third tarsomeres of both female and male leg pairs (Fig. 1A, G). The setal shaft is straight, 80.25 ± 1.68 ($n = 10$) μm in length and 3.13 ± 0.16 ($n = 10$) μm in width. Each seta had a spatulate and broad terminal plate (Fig. 1D, I). The widest part of the terminal plate was 10.38 ± 0.24 ($n = 10$) μm in width. The ventral and dorsal surfaces of the terminal plate were both smooth. The density of the spatulate setae was 0.93 ± 0.12 ($n = 10$) setae per 100 μm^2 area on average.

Discoidal setae were found only in the center of the first and second tarsomeres of the male forelegs and mesolegs and were absent on female legs (Fig. 1A, E, F). The setal shaft was straight, 75.63 ± 3.48 ($n = 10$) μm in length and 4.29 ± 0.20 ($n = 10$) μm in width. Each seta had a round to oval-shaped terminal plate. The terminal plate is 10.24 ± 0.35 ($n = 10$) μm in the long diameter and 8.47 ± 0.27 ($n = 10$) μm in the short diameter. The density of the discoidal setae was 0.73 ± 0.08 ($n = 10$) per 100 μm^2 area on average.

Three-dimensional topography of the terminal plates of adhesive setae. With SEM, we can obtain the ultrastructure of adhesive setae, but the images of SEM remain only two dimensional. The three-dimensional topography of the terminal plates of three types of adhesive setae (pointed, spatulate, and discoidal) were

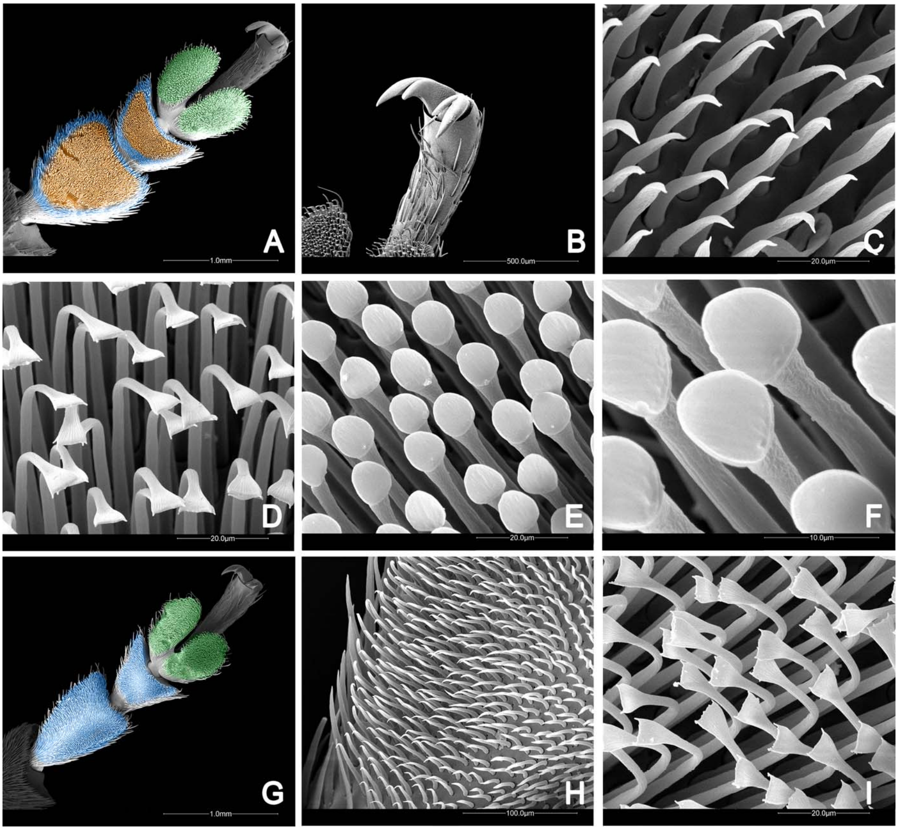

Fig. 1. Ultrastructure of the tarsus and adhesive setae of *Chrysochus chinensis*. (A) Front tarsus of male, ventral side. (B) An ungue of male. (C) Pointed setae of male. (D) Spatulate setae of male. (E, F) Discoidal setae of male. (G) Front tarsus of female, ventral side. (H) Pointed setae of female. (I) Spatulate setae of female. Blue indicates the distribution of the pointed setae, green indicates the distribution of the spatulate setae, orange indicates the distribution of the discoidal setae.

imaged and measured with AFM. The height of investigated materials must be limited to <12 µm across the *z*-axis for Dimension ICON. The length of the setae upright onto the tarsus extended far beyond the range in the *z*-axis, causing the tested seta to move even under very little pressure and would lead to unstable and unrepeatable images. To avoid this, a single seta was positioned and mounted on a glass slide so that the range in the *z*-axis was reduced to $<2{,}500$ nm.

The three-dimensional topography of the terminal plate surface was recorded at a high spatial resolution (256×256) with AFM. Both the ventral side and the dorsal side of the terminal plate of the three types of setae were scanned in our experiment. As shown in Fig. 2, the ventral side of the pointed seta was narrow and the center part was slightly raised (Fig. 2A). The dorsal side of the pointed

Table 1. Measurements of the three types of adhesive setae of *Chrysochus chinensis*.

Adhesive Setae	**Measurements**		
	Pointed setae	**Spatulate setae**	**Discoidal setae**
Number of setae per unit area (no./100 μm^2)	0.97 ± 0.09 ($n = 10$)	0.93 ± 0.12 ($n = 10$)	0.73 ± 0.08 ($n = 10$)
Length of seta (μm)	82.01 ± 1.71 ($n = 10$)	80.25 ± 1.68 ($n = 10$)	75.63 ± 3.48 ($n = 10$)
Diameter of setal shaft (μm)	3.24 ± 0.12 ($n = 10$)	3.13 ± 0.16 ($n = 10$)	4.29 ± 0.20 ($n = 10$)
Area of a terminal plate (μm^2)	7.59 ± 1.76 ($n = 10$)	41.16 ± 1.46 ($n = 10$)	63.65 ± 2.35 ($n = 10$)
Length of a terminal plate (μm)	4.76 ± 0.26 ($n = 10$)	10.38 ± 0.24 ($n = 10$)	10.24 ± 0.35 ($n = 10$)
Width of a terminal plate (μm)	4.32 ± 0.22 ($n = 10$)	7.31 ± 0.20 ($n = 10$)	8.47 ± 0.27 ($n = 10$)

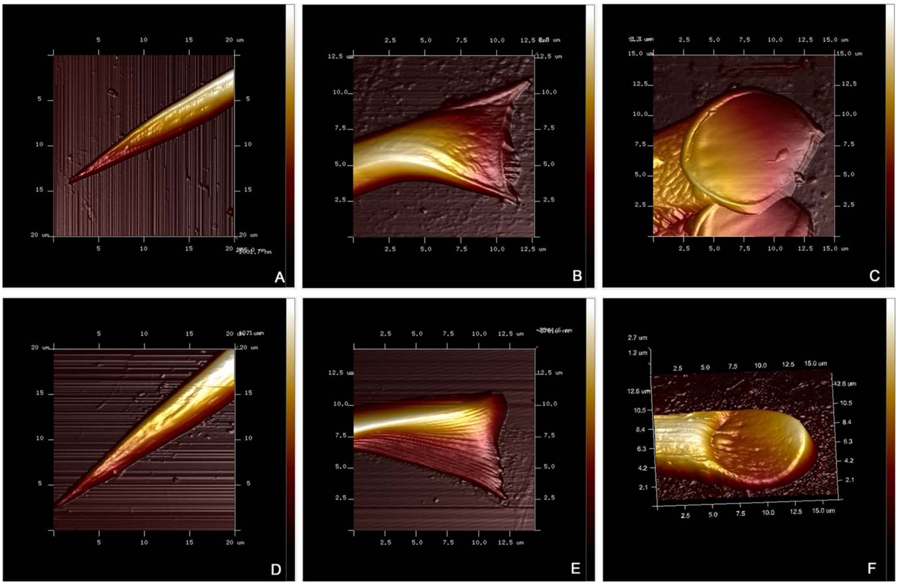

Fig. 2. Three-dimensional topography of the terminal plate of a single adhesive seta of *Chrysochus chinensis*. (A) Ventral side of a pointed seta. (B) Ventral side of a spatulate seta. (C) Ventral side of a discoidal seta. (D) Dorsal side of a pointed seta. (E) Dorsal side of a spatulate seta. (F) Dorsal side of a discoidal seta.

seta was smooth (Fig. 2D). The ventral side of the spatulate seta was triangular and smooth with a short edge at two sides of the terminal plate. The edge was about 200 nm high (Fig. 2B). The spatulate seta had rows of shallow longitudinal ridges on its dorsal surface and the sides were about 100 nm high (Fig. 2E). The surface topography of the ventral side of the discoidal seta was slightly concave in the main part of the terminal plate with a circular and high edge (Fig. 2C). The edge of the discoidal seta is 200–400 nm higher than the center. The surface topography of the dorsal side of the discoidal seta was smooth and its tip lifted a little in front (Fig. 2F). There was a boundary between the terminal plate and its setal shaft. The images obtained were stable and the trace and retrace height profiles at the same position were similar. Vertical movement of the *z*-piezo ranged from 0 to 2,361 nm.

Ultrastructure of the elytra epidermis of *Ch. chinensis*. According to our observations, during mating, males usually remained on the back of females. They grabbed the edge of female elytra with the sharp ungues and adhered to the female elytra epidermis with the tarsal ventral side. It was quite difficult to separate them. We examined the elytra ultrastructures of female *Ch. chinensis* using SEM and found that there were many tiny holes uniformly distributed on the elytra; the other part of the elytra was smooth without special structures. We examined the elytra ultrastructures of female Ch. chinensis using SEM and found that there were many tiny holes uniformly distributed on the elytra; the other part of the elytra was smooth without special structures (Fig. 3). The density of the holes was approximately 11/0.25 mm^2 ($n = 5$)

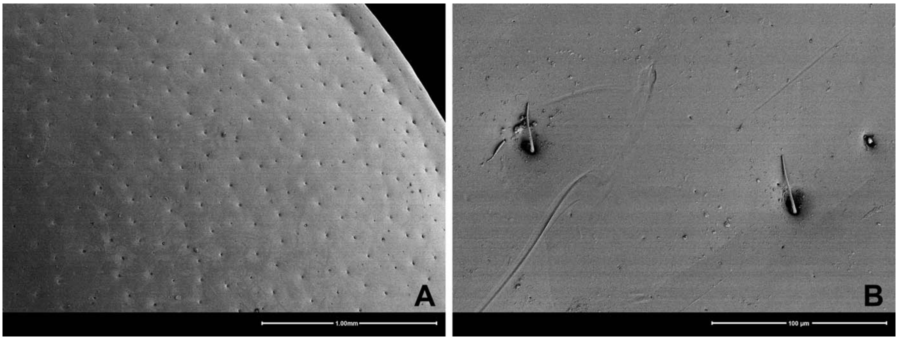

Fig. 3. Ultrastructure of the elytra epidermis of female *Chrysochus chinensis*. A. Dorsal view of the elytra. B Hairs on the elytra.

and the average distance between two adjacent holes was 136.53 ± 11.81 μm. The distance was much larger than the size of adhesive setae. There was a spine in each hole, which was 31.80 ± 5.00 μm ($n = 5$) long.

Discussion

This research aimed to provide the two-dimensional ultrastructure and three-dimensional topography of the micron-scale adhesive setae in *Ch. chinensis* and to explore the mechanism of attachment. According to our results, *Ch. chinensis* had three types of adhesive setae, pointed, spatulate, and discoidal, on the ventral side of the first to the third tarsomeres. The pointed and spatulate setae were on both female and male beetles, whereas the discoidal setae were observed only on males. Our result showed that the terminal plate of the discoidal seta had a concave center and a high edge (200–400 nm higher than the center). This structure was more likely to gather and hold a 200- to 400-nm-thick layer of liquid film between the terminal plate's surface and the substrate. The fluid film could provide a capillary force to enhance the foot adhesion force.

In contrast to geckoes and spiders, which use a "dry adhesion" mechanism in which the adhesion force is Van der Waals force (Arzt et al. 2003; Autumn et al. 2000, 2002; Huber et al. 2005), insects, including beetles, use a "wet adhesion" mechanism. They adhere to substrates with the additional aid of fluid film that is secreted by gland cells under epidermis of the tarsus (Betz 2003). The secretion droplet volume of ladybird beetles reduced to 65% within 1 h, suggesting comparatively stable compounds in the beetle fluid (Peisker and Gorb 2012). The topography (a concave center and a higher edge) of the discoidal seta terminal plate was a suitable structure for wet adhesion. For the beetle's micron-scale setae, the function of capillary force plays a more significant role than Van der Waals force, although on a submicron scale or nanoscale spatula of gecko's toe hairs, Van der Waals interaction is no longer negligible and can compete with the capillary force (PGeim at al. 2003).

Numerous studies have shown that many insects have excellent adhesion abilities on smooth substrates, including artificial and natural substrates (Edwards 1982; Eigenbrode 1996, 1999; Federle et al. 2002; Stork 1980). For insects using an attachment mechanism based on hairy structures, the strong attachment ability to smooth surface is based on the maximized real contact area between the foot and surfaces (Kesel et al. 2004, Ruibal and Ernst 1965). However, usually the surfaces in the natural environment are not absolutely smooth, rather than slightly structured in the microscale. "Slightly structured" means that the surfaces have a microtexture. The claws cannot sufficiently catch the substrate, and a normal foot cannot contact the substrate completely because there are some micron-scale gaps on slightly structured surfaces. It is easier for the smaller setal terminal plates to insert into the gaps of a slightly structured surface and to obtain a real contact area (Bullock and Federle 2011a). The miniaturized contact elements of the attachment apparatus and numerous hairs can provide sufficient adhesion forces (Autumn et al. 2000).

According to our results, the three types of setae of *Ch. chinensis* had tiny terminal plates. The pointed setae had the smallest terminal plates (7.59 ± 1.76 μm^2) and the spatulate setae had middle-sized terminal plates (41.16 ± 1.46 μm^2), compared with the largest terminal plate (63.65 ± 2.35 μm^2) in discoidal setae. Although compared with a discoidal seta the pointed seta and the spatulate seta have smaller terminal plate areas and the adhesion force of each seta is subsequently weaker, it can still provide sufficient adhesion force when the small setae are able to move into the gaps and every terminal plate can contact the substrate completely. To do so, the setae need to be quite small and be in large numbers. In addition to adhesion forces, they also can supply a strong friction to hold the body from dropping (Bullock and Federle 2011a). The function of both tapered and spatulate setae is for climbing (Stork 1980), but they produce more friction rather than adhesion (Bullock and Federal 2011a).

The discoidal seta of the male *Ch. chinensis*, which is very common on most male leaf beetles, is a good model for artifically imitating. The discoidal setae have the biggest terminal plate area (63.65 ± 2.35 μm^2). The surface topography of the expanded terminal plate directly affects the adhesion force. The topography of discoidal setae can gather liquid and produce a 200- to 400-nm-thick layer of fluid film between the terminal plate and smooth substrates. With the help of capillary force of the tarsal secretion, it can provide a strong adhesion force. On a smooth surface, such as the smooth female elytra, the real contact area of a discoidal seta is approximately equal to the terminal plate area, so this type of seta might be more suitable for smooth surfaces.

In our observation of mating behavior, the male beetles used the fore- and mesolegs to tightly latch onto the elytra of female beetles. The function of the discoidal seta, which is only present on the fore- and mesolegs of male beetles, is to serve for strong attachment force during mating and, thus, it is also called "sex seta" (Stork 1980). Most parts of the elytral epidermis were quite smooth; the distance of the holes on the elytra were much larger than the length of the discoidal, spatulate, or tapered terminal plates. Thus, most of the terminal plates could contact the smooth elytra completely. We hypothesized that the discoidal seta might be a functional structure adapting to the female elytral surface.

Factors that affect adhesion force are complicated, such as contact area, surface topography, number of adhesive setae, secretion and capillary force, softness of setal materials, length of setal shafts, and even the incline angle of the terminal plate surface.

Conclusion

The surface topography of the discoidal seta was slightly concave in the main part of the terminal plate with circular and high edges. This topography can more easily gather liquid and produce a 200- to 400-nm-thick layer of fluid film. With the help of the capillary force produced by the secretion of tarsal gland cells, it can provide strong adhesion force. For the beetle's micron-scale setae, the function of capillary force plays a more significant role than Van der Waals force. The discoidal setae, which exist only in male beetles, may play roles in the mating process as the tarsi of male fore- and mesolegs were observed contacting the surface of the female beetle's elytra while mating. Although the terminal plates of tapered and spatulate setae were relatively smaller and the ability of collecting fluid film is weaker compared with discoidal seta, the discoidal seta could more easily insert into the gaps of a slightly rough surface and be more suitable for the slightly rough natural environment such as host plants. Complicated factors, including the real contacting area, number of adhesive setae, surface topography, secretion, and capillary force, can affect the adhesion force.

Acknowledgments

We are grateful to Yunsheng Lin (Institute of Electrical Engineering, Chinese Academy of Sciences) for providing technical assistance with the AFM. This work was supported by the following sources: the National Natural Science Foundation of China (grant no. 32070470), the Science and Technology Research Youth Fund of Colleges and Universities in Hebei Province (grant no. QN2020261), the National Basic Research Program of China (973 Program) (grant no. 2011CB302102), and the Biodiversity Survey and Assessment Project of the Ministry of Ecology and Environment, China (grant no. 2019HJ2096001006).

References Cited

Arzt, E., S. Gorb and R. Spolenak. 2003. From micro to nano contacts in biological attachment devices. Proc. Natl. Acad. Sci. USA 100 (29): 10603–10606.

Autumn, K., Y.A. Liang, S.T. Hsieh, W. Zesch, W. P. Chan, T. W. Kenny, R. Fearing and R. J. Full. 2000. Adhesive force of a single gecko foot-hair. Nature 405: 681–685.

Autumn, K., M. Sitti, Y.A. Liang, A.M. Peattie, W.R. Hansen, S. Sponberg, T.W. Kenny, R. Fearing, J.N. Israelachvili and R.J. Full. 2002. Evidence for van der waals adhesion in gecko setae. Proc. Natl. Acad. Sci. USA 99: 12252–12256.

Betz, O. 2003. Structure of the tarsi in some *Stenus* species (Coleoptera, Staphylinidae): external morphology, ultrastructure, and tarsal secretion. J. Morphol. 255 (1): 24–43.

Beutel, R.G. and S.N. Gorb. 2001. Ultrastructure of attachment specializations of hexapods (Arthropoda): Evolutionary patterns inferred from a revised ordinal phylogeny. J. Zool. Syst. Evol. Res. 39: 177–207.

Braet, F., R. de Zanger, C. Seynaeve, M. Baekeland and E. Wisse. 2001. A comparative atomic force microscopy study on living skin fibroblasts and liver endothelial cells. J. Electron Microsc. 50: 283–290.

Braet, F., C. Seynaeve, R. de Zanger and E. Wisse. 1998. Imaging surface and submembranous structures with the atomic force microscope: A study on living cancer cells, fibroblasts and macrophages. J. Microsc. 190: 328–338.

Bullock, J.M.R. and W. Federle. 2011a. The effect of surface roughness on claw and adhesive hair performance in the dock beetle *Gastrophysa viridula*. Insect Sci. 18: 298–304.

Bullock, J.M.R. and W. Federle. 2011b. Beetle adhesive hairs differ in stiffness and stickiness: In vivo adhesion measurements on individual setae. Sci. Nat. 98 (5): 381–387.

Edwards, P.B. 1982. Do waxes on juvenile Eucalyptus leaves provide protection from grazing insects? Aust. J. Ecol. 7: 347–352.

Eigenbrode, S.D., T. Castagnola, M.B. Roux, L. Steljes. 1996. Mobility of three generalist predators is greater on cabbage with glossy leaf wax than on cabbage with a wax bloom. Entomol. Exp. appl. 81: 335–343.

Eigenbrode, S.D., N.N. Kabalo, K.A. Stoner. 1999. Predation, behavior, and attachment by *Chrysoperla plorabunda* larvae on *Brassica oleracea* with different surface waxblooms. Entomol. Exp. Appl. 90: 225–235.

Eisner, T. and D.J. Aneshansley. 2000. Defense by foot adhesion in a beetle (*Hemisphaerota cyanea*). Proc. Natl. Acad. Sci. USA 97: 6568–6573.

Federle, W., E.L. Brainerd, T.A. McMahon and B. Hölldobler. 2001. Biomechanics of the movable pretarsal adhesive organ in ants and bees. Proc. Natl. Acad. Sci. USA 98 (11): 6215–6220.

Federle, W., M. Riehle, A.S.G. Curtis and R.J. Full. 2002. An integrative study of insect adhesion: Mechanics and wet adhesion of pretarsal pads in ants. Integr. Comp. Biol. 42: 1100–1106.

Geim, A.K., S.V. Dubonos, I.V. Grigorieva, K.S. Novoselov, A.A. Zhukov and S.Y. Shapoval. 2003. Microfabricated adhesive mimicking gecko foot-hair. Nat. Mater. 2 (7): 461.

Goodwyn, P.P., A. Peressadko, H. Schwarz, V. Kastner and S. Gorb. 2006. Material structure, stiffness, and adhesion: Why attachment pads of the grasshopper (*Tettigonia viridissima*) adhere more strongly than those of the locust (*Locusta migratoria*) (Insecta: Orthoptera). J. Comp. Physiol. A 192: 1233–1243.

Gorb, E.V. and S.N. Gorb. 2002. Attachment ability of the beetle *Chrysolina fastuosa* on various plant surfaces. Entomol. Exp. Appl. 105: 13–28.

Gorb, S.N. 1998. The design of the fly adhesive pad: Distal tenent setae are adapted to the delivery of an adhesive secretion. Proc. Royal Soc. B 265: 747–752.

Gorb, S.N. 2001. Attachment devices of insect cuticle. Kluwer Academic Publishers, Dordrecht, the Netherlands.

Gorb, S.N. and R.G. Beutel. 2001. Evolution of locomotory attachment pads of hexapods. Naturwissenschaften. 88 (12): 530–534.

Huber, G., S.N. Gorb, R. Spolenak and E. Arzt. 2005. Resolving the nanoscale adhesion of individual gecko spatulae by atomic force microscopy. Biol. Lett. 1: 2–4.

Jiang, S.Q. 1980. The life habits and rearing method of *Chrysochus chinensis* Baly (Coleoptera: Chrysomelidae). Entomol. Sci. 5: 214–215.

Kesel, A.B., A. Martin and T. Seidl. 2004. Getting a grip on spider attachment: An AFM approach to microstructure adhesion in arthropods. Smart Mater. Struct. 13: 512–518.

Liu, Z. and A.P. Liang. 2013. Ultrastructure of the tarsus in *Oides decempunctatus* (Billberg) (Coleoptera: Chrysomelidae). J. Kans. Entomol. Soc. 86 (2): 122–132.

Orivel, J., M.C. Malherbe and A. Dejean. 2001. Relationships between pretarsus morphology and arboreal life in ponerine ants of the genus *Pachycondyla* (Formicidae: Ponerinae). Ann. Entomol. Soc. Am. 94 (3): 449–456.

Peisker, H. and S.N. Gorb. 2012. Evaporation dynamics of tarsal liquid footprints in flies (*Calliphora vicina*) and beetles (*Coccinella septempunctata*). J. Exp. Biol. 215: 1266–1271.

Pelletier, Y. and Z. Smilowitz. 1987. Specialized tarsal hairs on adult male Colorado potato beetles, *Leptinotarsa decemlineata* (Say), hamper its locomotion on smooth surfaces. Can. Entomol. 119(12): 1139–1142.

Pettinger, B., N. Erina and C. Su. 2010. Quantitative mechanical property mapping at the nanoscale with Peak Force QNM. Bruker Appl. Note 128: 1–12.

Ruibal, R. and V. Ernst. 1965. The structure of the digital setae of lizards. J. Morphol. 117: 271–94.

Stork, N.E. 1980. A scanning electron microscope study of tarsal adhesive setae in the Coleoptera. Zool. J. Linn. Soc. 68: 173–306.

Stork, N.E. and M.E.G. Evans. 1976. Tarsal setae in Coleoptera. Int. J. Insect Morphol. Embryol. 5: 219–221.

Tian, D.L., J. Tooker, M. Peiffer, S.H. Chung and W. Gary. 2012. Felton role of trichomes in defense against herbivores: Comparison of herbivore response to woolly and hairless trichome mutants in tomato (*Solanum lycopersicum*). Planta 236: 1053–1066.

van Casteren, A. and J.R. Codd. 2010. Foot morphology and substrate adhesion in the Madagascan hissing cockroach, *Gromphadorhina portentosa*. J. Insect Sci. 10 (40): 1–12.

Vogel, M.J. and P.H. Steen. 2010. Capillarity-based switchable adhesion. Proc. Natl. Acad. Sci. USA 107 (8): 3377–3381.

Walker, G. 1993. Adhesion to smooth surfaces by insects—A review. Int. J. Adhes. Adhes. 13 (1): 3–7.

Weirauch, C. 2007. Hairy attachment structures in Reduviidae (Cimicomorpha, Heteroptera), with observations on the fossula spongiosa in some other Cimicomorpha. Zool. Anz. 246: 155–175.

Wigglesworth, V.B. 1987. How does a fly cling to the under surface of a glass sheet? J. Exp. Biol. 129: 373–376.

Yu, P.Y., Y.S. Wang and X.K. Yang. 1996. Economic Insect Fauna of China. Fasc. 54. Coleoptera: Chrysomeloidea (II). Science Press, Beijing, pp. 8–11.